

Harmonic and anharmonic properties of Fe and Ni: Thermal expansion, exchange-correlation errors, and magnetism

Alison J. Hatt and Brent C. Melot

Materials Department, University of California, Santa Barbara, California 93106, USA

Shobhana Narasimhan

Theoretical Sciences Unit, Jawaharlal Nehru Centre for Advanced Scientific Research, Jakkur, Bangalore 560064, India

(Received 4 August 2009; revised manuscript received 13 September 2010; published 12 October 2010)

We have investigated the source of errors in *ab initio* calculations of thermal properties of the magnetic metals Fe and Ni and their dependence on the form of the exchange and correlation functional. We used density-functional theory and density-functional perturbation theory together with the quasiharmonic approximation to compute the coefficient of thermal expansion, bulk modulus and its pressure derivative, phonon modes, and Grueneisen parameters of bcc Fe and fcc Ni. In nonmagnetic metals the main source of error in calculated thermal properties can be attributed to evaluation of properties at incorrect lattice constants, which in turn may be traced to the choice of exchange and correlation functional. However, for magnetic metals the properties may be evaluated at both incorrect lattice constant and incorrect magnetic moment. This affects vibrational properties so that it is no longer true that anharmonic errors are significantly less than errors at harmonic order.

DOI: [10.1103/PhysRevB.82.134418](https://doi.org/10.1103/PhysRevB.82.134418)

PACS number(s): 71.15.Mb, 65.40.-b

I. INTRODUCTION

The development of density-functional theory (DFT) has enabled the calculation of crystal properties from first principles. Though, in principle, such calculations could be exact, the precise form of the exchange and correlation (XC) interaction between electrons is not known. Therefore, in practice, the accuracy of any DFT calculation depends on the choice of XC functional used. It has been suggested¹ that such XC errors may be expected to increase with temperature, and thus may contribute significantly to errors in computed thermodynamic properties. There are other sources of possible error at finite temperatures: due to the presence of phonon-phonon interactions, the lattice constant of a crystal changes with temperature. This anharmonic effect is frequently treated within the quasiharmonic approximation,^{2,3} whose validity may break down at high temperatures. Finally, in magnetic materials, there are additional effects due to the disordering of magnetic moments as temperature is increased; the effects of this are not well understood and are difficult to treat theoretically. In this paper, we attempt to investigate the systematics of the errors introduced by these factors in the calculated thermal properties of the ferromagnetic metals Fe and Ni.

The two most commonly used forms of the XC functional are the local (spin)-density approximation or L(S)DA and the generalized gradient approximation (GGA). (In the rest of this paper, when we refer to the LDA or GGA, we will implicitly be referring to their spin polarized versions.) They have been widely tested and found to give good results in many systems. However, it is often hard to decide, beforehand, which of these two functionals may be expected to perform better in a given situation. The LDA usually overbinds, leading (most of the time) to lattice constants that are too small, while the GGA leads frequently (but not always) to lattice constants that are too high.

There have been few studies of the implications and variation in this over/underbinding as a function of temperature. In a study of the thermal properties of copper, Narasimhan and de Gironcoli speculated that computational errors in a variety of measurable thermal properties may be traced back to the error made in computing the equilibrium lattice parameter at zero temperature, $a_0(0)$. One consequence of this is that the XC errors in calculated anharmonic properties are considerably less than in the corresponding harmonic properties. Another consequence of this is that the under(over)estimation of $a_0(0)$ by the LDA (GGA) leads to a value of the bulk modulus, $B_0(0)$, that is too high (low). The combination of these two effects results in too low (high) a value for the coefficient of thermal expansion, $\alpha(T)$. Thus, a low (high) $a_0(T)$ may be expected to always be accompanied by a low (high) $\alpha(T)$, leading to an increasing error in $a_0(T)$ and other quantities dependent on this, as the temperature is increased. The authors suggested that these features may hold true for a wide variety of materials.

In recent work, Grabowski *et al.*⁴ have demonstrated that these arguments are applicable to other metals: in addition to Cu, they have studied the nonmagnetic face-centered-cubic (fcc) metals Al, Pb, Ag, Au, Pd, Pt, Rd, and Ir. In most cases, they found that the LDA (GGA) does indeed find lattice constants that are too small (large) and bulk moduli that are too high (low), at zero temperature. The exceptions are Pt and Au, where the LDA gets the lattice constant almost exactly right. Similarly, in most cases the LDA (GGA) finds phonon frequencies that are higher (lower) than experiment. An examination of their data also reveals that ΔB_0 , the discrepancy between the LDA and GGA values of B_0 , a harmonic quantity, is much larger than $\Delta B'_0$, the discrepancy between the LDA and GGA values of the corresponding anharmonic quantity, the pressure derivative of the bulk modulus, B'_0 . $\Delta B'_0$ is typically an order of magnitude smaller than ΔB_0 . Their results for $\alpha(T)$ are also in keeping with the

trends predicted by Narasimhan and de Gironcoli: (i) in most cases the LDA (GGA) gives values of $\alpha(T)$ that are too low (high), (ii) for Pt, where the LDA gets a_0 exactly correct, it also gets $\alpha(T)$ in agreement with experiment, and (iii) for Au, where LDA gets a_0 very slightly too large, it slightly overestimates $\alpha(T)$, while the GGA error in $\alpha(T)$ is considerably larger.

This line of investigation has thus far been limited to non-magnetic metals. In the present work we examine the case of two elemental ferromagnetic materials, body-centered-cubic (bcc) Fe and fcc Ni, to determine whether the same trends are present and to illuminate the effects of magnetic order on the calculation of thermal properties. Specifically, we want to know if the relative accuracy of harmonic and anharmonic properties, as calculated with GGA and LDA, may be predicted by the accuracy of the zero temperature lattice parameter. The presence of magnetic moments complicates the situation by increasing the dimensionality of the phase space in which minima of the (free) energy landscape have to be determined, i.e., the equilibrium structure now corresponds to a minimum with respect to both coordinate and spin degrees of freedom. Moreover, there can be a significant interplay between the degrees of freedom corresponding to spins and lattice parameters. It is well known that larger lattice constants promote an increased degree of spin polarization, and that the presence of ferromagnetism tends to favor an expansion of the lattice. Finite temperature properties also depend on the behavior of phonons, and it has been demonstrated recently that there can be strong interactions between phonons and magnetism.⁵⁻⁷

An improved understanding of the sources and magnitudes of errors in the thermodynamic properties of magnetic materials could conceivably play a role in resolving several long-standing puzzles of scientific and technological interest, such as the debate over the properties of the earth's magnetic core, or the precise origin of the Invar effect in the thermal expansion of magnetic alloys.^{8,9}

II. METHODS

The quasiharmonic approximation separates the free energy into a static and a dynamic part. In order to evaluate these, we use DFT and density-functional perturbation theory (DFPT) as implemented in the PWSCF and PHONON packages of the QUANTUM ESPRESSO distribution.¹⁰ The calculations are carried out making use of the spin-polarized (SP) form of the Kohn-Sham equations. Unless otherwise mentioned, the magnetic moment is allowed to vary freely so as to minimize the total energy; some calculations to extract trends are however carried out using the constrained moment approach. We use ultrasoft pseudopotentials (USPPs) and a plane-wave basis with a kinetic-energy cutoff of 25 Ry for Fe and 40 Ry for Ni, along with increased cutoffs of 200 Ry and 320 Ry, respectively, for the augmentation charges associated with the USPPs. For the LDA we use the Perdew-Zunger form¹¹ and for the GGA we use the form given by Perdew, Burke, and Ernzerhof,¹² with nonlinear core corrections in both cases.¹³ Brillouin zone (BZ) integrations involved in computing the total (static) energy E_{stat} are performed with $10 \times 10 \times 10$

and $6 \times 6 \times 6$ Monkhorst-Pack meshes for bcc Fe and fcc Ni, respectively, along with a Methfessel-Paxton smearing scheme with widths of 0.02 Ry and 0.01 Ry. All these parameters have been chosen so as to ensure that the values of a_0 , B_0 , B'_0 and phonon frequencies are well converged.

In order to compute properties at finite temperatures using the quasiharmonic approximation, one needs to know how the vibrational frequencies $\omega_{\mathbf{q}\lambda}$ vary with lattice constant a ; here \mathbf{q} denotes the phonon wave vector, and λ the phonon branch. DFPT calculations are carried out for a number of values of a , and for values of \mathbf{q} corresponding to a $4 \times 4 \times 4$ Monkhorst-Pack grid in the first BZ. Phonon frequencies at other values of \mathbf{q} are then obtained by Fourier interpolation, and at other (intermediate) values of a by a three-point interpolation formula. All vibrational properties that involve a sum over the BZ are evaluated using interpolated values on a finer $10 \times 10 \times 10$ grid. The free energy at temperature T and lattice constant a is then given by

$$F(a, T) = E_{stat}(a) + k_B T \sum_{\mathbf{q}\lambda} \ln \left\{ 2 \sinh \left[\frac{\hbar \omega_{\mathbf{q}\lambda}(a)}{2k_B T} \right] \right\}. \quad (1)$$

Here, the second term on the right-hand side is the vibrational free energy; in the present work, we neglect the contribution from the electronic free energy, as it is expected to be small. The sum is over all three phonon branches λ and over all wave vectors \mathbf{q} in the BZ, \hbar is the Planck constant and k_B is the Boltzmann constant. By fitting the Murnaghan equation of state (EOS) (Ref. 14) to $F(a, T)$ at a given temperature, we obtain the equilibrium lattice parameter a_0 , bulk modulus B_0 , and pressure derivative of the bulk modulus B'_0 , all as functions of temperature T . Once the temperature dependence of the lattice constant is known, one can then also compute how phonon frequencies (ω) and mode Grüneisen parameters (γ) vary with temperature [through their dependence on $a_0(T)$], as well as the coefficient of thermal expansion $\alpha(T)$.

III. RESULTS AND DISCUSSION

A. Results at room temperature

In Table I, we give the calculated values at a temperature $T=300$ K, of a_0 , B_0 , $B'_0(T)$, α , γ_{avg} , ω_{avg} , and m . Here, avg indicates an averaging over all wave vectors \mathbf{q} and branches λ , weighted by Bose-Einstein occupation factors. The corresponding experimental values, where available, are also given. Note that, for both Fe and Ni, the GGA value for a_0 lies very close to the experimental value while LDA underestimates the lattice constant: by 3.8% for Fe and by 2.6% for Ni. This behavior is quite different from that seen for the other metals mentioned in Sec. I, where the experimental value of a_0 lies either sandwiched between the LDA and GGA values or, in the case of Au and Pt, very close to the LDA value. If the arguments mentioned in Sec. I apply to these ferromagnetic metals, one would expect that the GGA, having more accurately predicted a_0 , should perform considerably better than the LDA in evaluating the elastic and thermal properties as well.

Comparing calculated and experimental values for both Fe and Ni (see Table I), we find significantly smaller errors

TABLE I. Calculated and experimental values, at room temperature, of the equilibrium lattice parameter a_0 , bulk modulus B_0 , pressure derivative of the bulk modulus B'_0 , the coefficient of thermal expansion α , average phonon frequency ω_{avg} , average Grueneisen parameter γ_{avg} and magnetization for Fe and both spin polarized (SP) and nonspin polarized (NSP) Ni. NSP values are not given for Fe due to unstable phonon modes in nonmagnetic bcc Fe. Experimental values are from Refs. 15–18.

	a_0 (Å)	B_0 (GPa)	B'_0	$\alpha \times 10^{-6}$	ω_{avg} (cm^{-1})	γ_{avg}	m (μ_B/atom)
Fe							
LDA	2.76	213	5.59	7.39	222	1.28	2.07
GGA	2.87	142	4.8	11.6	209	1.88	2.44
Expt.	2.87	168	5.29	11.6			2.22
Ni, SP							
LDA	3.43	230	5.47	10.0	210	1.90	0.51 ^a
GGA	3.54	177	5.27	11.8	190	1.91	0.69 ^a
Expt.	3.52	186	5.2	12.7			0.61
Ni, NSP							
LDA	3.43	238	5.08	10.5			
GGA	3.53	186	5.57	12.0			

^aReference 19.

in B_0 and α with GGA than LDA. This is not true for B'_0 ; however, experimental values for this quantity typically involve rather large error bars and so the comparison may be less meaningful.

The LDA and GGA values of magnetization $m_0(0)$ are also found to differ significantly. For Fe, the experimental value of 2.22 μ_B per atom lies sandwiched between the LDA and GGA values of 2.07 μ_B and 2.44 μ_B , respectively. Similarly, for Ni, the LDA and GGA values are 0.51 μ_B and 0.69 μ_B , respectively,¹⁹ while the experimental value is 0.61 μ_B .

We now consider the discrepancy between LDA and GGA values of the calculated properties, denoted by Δ . For Fe, ΔB_0 is 40%, which is indeed larger (though not by an order of magnitude) than the value of 15% for $\Delta B'_0$. For Ni the value of $\Delta B_0=26\%$ is much larger than $\Delta B'_0=3.7\%$. Thus, the trend exhibited by the nonmagnetic metals, where the discrepancies in all anharmonic quantities are considerably less than the discrepancies in the corresponding harmonic quantities, still holds for the magnetic metals, though to a lesser extent.

Finally, we look for this trend in comparison of $\Delta\omega_{avg}$, a harmonic quantity, with $\Delta\gamma_{avg}$, the corresponding anharmonic quantity. For Fe, the former has a value of 6%, which is much less than the value of 38% for the latter, and so the trend is reversed. However, we find that it holds for Ni in which $\Delta\omega_{avg}=10\%$ and $\Delta\gamma_{avg}=0.5\%$.

Some insight into the reasons why these magnetic metals behave so differently from the nonmagnetic metals can be obtained from looking at the plots of phonon frequencies and Grueneisen parameters. For the nonmagnetic metals, the primary effect upon going from the LDA to the GGA is an increase in lattice constant and a corresponding decrease in force constants, which scale inversely as a high (8–10)

power of bond lengths.^{20,21} As a result, the GGA graphs of phonon dispersion curves look essentially like a scaled version of the LDA curves. However, this is not true for magnetic metals, especially not for Fe. In Fig. 1, we show the phonon dispersion curves along high-symmetry directions in the BZ for bcc Fe; our results are very similar to those obtained by previous authors.²³ It can be seen that the shape of the LDA and GGA curves is quite different, especially in the neighborhood of the N and H points due to the complicating factor of magnetic moments. This becomes even more evident upon examining Fig. 2, which shows the LDA and GGA values of the mode Grueneisen parameters γ through the BZ. The LDA and GGA curves bear very little resemblance to each other. It is important to note that even in areas of the BZ where the LDA and GGA phonon dispersion curves appear

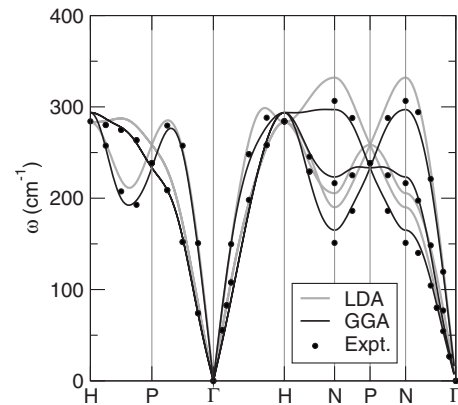


FIG. 1. Phonon dispersion for SP bcc Fe at room temperature, along high-symmetry directions. The dashed and solid curves represent LDA and GGA results, respectively. The dots are experimental points from Ref. 22.

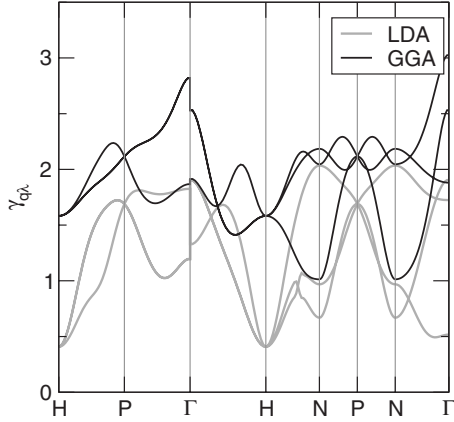


FIG. 2. Calculated Grueneisen parameters of SP Fe at room temperature. The gray and black curves represent LDA and GGA results, respectively.

qualitatively similar (for example, between P and Γ , N and P, or N and Γ) the mode Grueneisen parameters differ dramatically for the LDA and GGA, indicating that though the phonon frequencies may be close, the nature of the mode is quite different in the two cases. When there is such a large qualitative change, it is not meaningful to compute percentage discrepancies, and it is not surprising that $\Delta\gamma_{avg}$ is very large.

In Fig. 3, we have plotted the LDA and GGA phonon dispersion curves for Ni, at room temperature. Again our results are similar to those in Ref. 23 but with a small discrepancy due to the difference in a_0 at room temperature and 0 K. On looking at the dispersion one might be tempted to conclude that the LDA and GGA results produce qualitatively similar modes as the phonon frequencies appear to differ merely by a scaling factor. However, we have further calculated the Grueneisen parameters, shown in Fig. 4 which reveal that, as in the case of Fe, the nature of modes is actually quite different between the LDA and GGA, especially in the interior of the BZ, in the regions from K to Γ and from Γ to L.

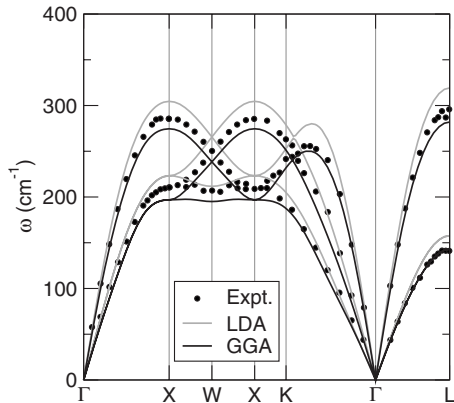


FIG. 3. Calculated phonons dispersion curves for SP Ni at room temperature, LDA. The gray and black curves represent LDA and GGA results, respectively. Experimental points from Ref. 24.

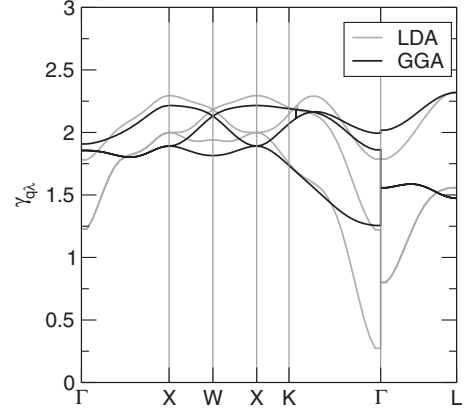


FIG. 4. Calculated values of Grueneisen parameters of SP Ni at room temperature. The gray and black curves represent LDA and GGA results, respectively.

B. Effect of magnetic moment on the equation of state

As mentioned in Sec. I, there is an interplay between magnetism on the one hand, and structure and elastic properties on the other hand. In order to examine this, we compare relaxed magnetization (RM) calculations for Fe to constrained magnetization (CM) calculations where the magnetic moment is fixed at a particular value.

As an example, we have plotted, in Fig. 5(a), both RM and CM results showing how the (static) total energy E varies with lattice constant a , using the GGA (qualitatively similar sets of curves are obtained on using the LDA). From an examination of this figure, the following points are evident: (i) the most favored magnetization varies with lattice constant, (ii) the magnetization increases with increasing lattice constant, and (iii) as a result of this, the bulk modulus is softened considerably when the magnetic moment is allowed to relax. This last point is manifested in the lower curvature of the RM curve, compared to that of any of the CM curves.

The interplay between magnetic moment and lattice constant is made evident in Fig. 5(b), which is extracted from the data contained in Fig. 5(a). The solid lines show how the magnetization varies when the lattice constant is held fixed, and the dashed lines show how the lattice constant varies when the magnetization is held fixed. In terms of Fig. 5(a), the former is comprised of points along the RM curve while the latter consists of points that lie at the minima of each of the CM curves [see, e.g., points in Fig. 5(a)]. The intersection of solid and dashed lines corresponds to the point that lies at the minimum of the RM curve. The solid lines in Fig. 5(b) show that the magnetization is increased when the lattice constant is increased. This can be understood in terms of the Stoner argument:²⁵ as a becomes larger, the bands become narrower and more highly peaked, and ferromagnetism is progressively favored as the lowering of energy from the exchange interaction prevails increasingly over the gain in band energy. The dashed lines in Fig. 5(b) show the complementary effect: a spin-polarized system would prefer to increase its interatomic spacing because the presence of aligned spins disfavors bonding. Note also that similar trends are exhibited by both the LDA and GGA.

By fitting the CM and RM curves to the Murnaghan EOS, we can see how magnetism affects elastic properties. The

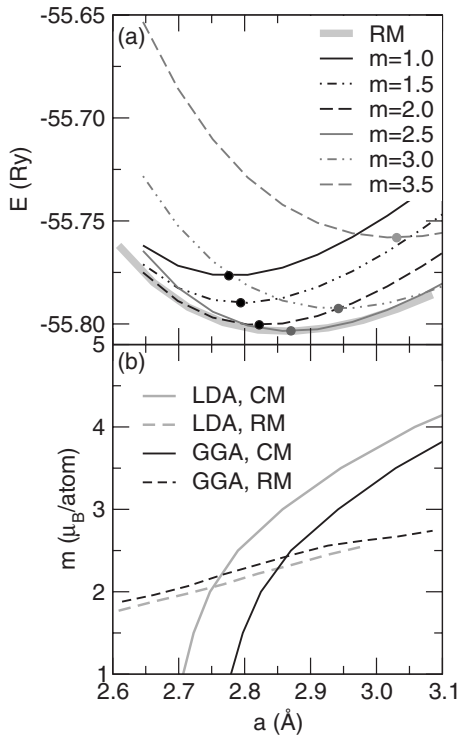


FIG. 5. Interplay between magnetic moments m and lattice constant a , for bcc Fe. (a) Total energy E as a function of a . Each curve corresponds to a different value of constrained magnetic moment, except for the bottommost (thick, gray) curve, which corresponds to the results when the magnetic moments are allowed to relax. The black dots indicate the minima of each CM curve. (b) Magnetic moment m as a function of lattice parameter a . Solid lines correspond to CM and minimized a ; dashed lines correspond to constrained a and RM.

dependence of B_0 and B'_0 (at $T=0$) on magnetization is shown in Fig. 6; the lines show the results from CM calculations while the symbols indicate the value obtained from the RM calculations. In Figs. 6(a) and 6(b), the symbols lie below and above the curves, respectively, i.e., the effect of allowing magnetization to relax is to soften the bulk modulus (as mentioned above), and also to make the EOS more anharmonic.

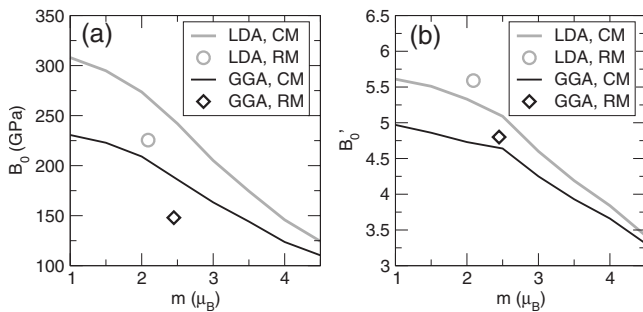


FIG. 6. Effect of magnetic moment on static elastic properties of Fe: the variation in (a) B_0 , the bulk modulus and (b) B'_0 , the pressure derivative of the bulk modulus, with magnetic moment m . The curves correspond to CM calculations while the symbols represent the result of an RM calculation.

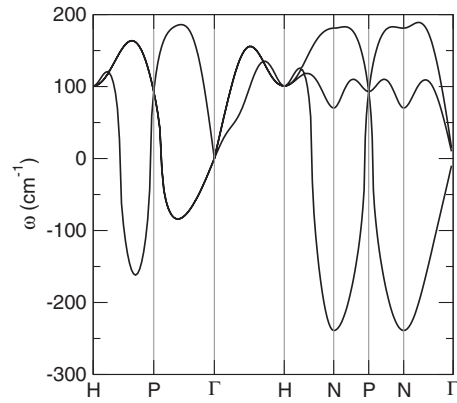


FIG. 7. Phonon dispersion curves for NSP bcc Fe, along high-symmetry directions, at $T=0$, obtained using GGA. A negative value for the frequency ω represents an imaginary frequency and thus an unstable mode, indicating the instability of the bcc structure for nonmagnetic Fe.

Similarly, one can study the effects of magnetization on phonon dispersion curves. For Ni, this has already been done by previous authors. While one set of authors,²³ upon comparing nonspin-polarized (NSP) and SP GGA calculations, concluded that magnetism has a negligible effect on phonon frequencies, a subsequent study⁶ concluded that this effect was not small. As expected, they found that near the zone boundary larger lattice constants lead to smaller frequencies; however, near the zone center the opposite effect is seen. We suggest that our results mentioned above, that the mode Grüneisen parameters look very different for the LDA and GGA, serve as a further example that magnetization can affect phonon modes.

The effect of vibrational properties on magnetism is exhibited more dramatically in Fe. In Fig. 7, we have plotted the phonon dispersion relations for Fe, obtained upon doing an NSP GGA calculation. In this figure, a negative value of ω indicates an imaginary frequency, i.e., an unstable mode. The presence of strongly unstable modes in the dispersion curve indicates that it is only the presence of magnetism that makes bcc Fe stable, as has been pointed out before.²⁶ In other words, just as the LDA and GGA SP curves for Fe are qualitatively different, so are the NSP and SP GGA curves, again indicating the presence of a strong coupling between magnetism and positional degrees of freedom.

C. Thermal expansion and temperature dependence

In Fig. 8, we compare our results for $\alpha(T)$, the linear coefficient of thermal expansion, with experimental data. As discussed in Sec. I, our experience with nonmagnetic metals leads us to postulate that errors in thermal and vibrational properties primarily arise from evaluating derivatives at an incorrect lattice constant, and hence the error in lattice constant was the primary contribution of error from the XC functional. Accordingly, in our results for Fe and Ni, we expect that the XC functional which more successfully predicts the lattice constant at $T=0$ should also obtain $\alpha(T)$ with greater accuracy. Up to a temperature of about 400 K for Fe, and 200 K for Ni, this is indeed so: we find that the GGA

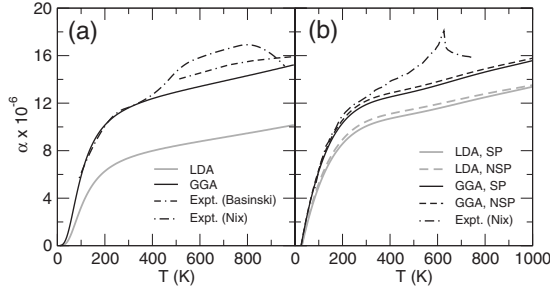


FIG. 8. Calculated values of the temperature dependence of the coefficient of thermal expansion α for (a) Fe and (b) Ni, obtained using the LDA and GGA. For Ni, results from both SP and NSP calculations are presented. The experimental values are from Refs. 15 and 16.

results are in excellent agreement with experiment. Above these temperatures (which are both roughly a third of the corresponding Curie temperatures), the experimental results from Nix and MacNair¹⁵ show a sudden departure from the low-temperature curves for both Fe and Ni, and diverge dramatically from the calculated values. However, slightly more recent experimental results on Fe from Basinski *et al.*¹⁶ do not show this behavior, and their results are similar to ours, although with somewhat higher values of α . This suggests that the high-temperature disagreement might be resolved by new, more accurate experimental measurements. This discrepancy above room temperature was also reported in Ref. 27 for linear-response calculations on Fe.

Also plotted in Fig. 8(b) for Ni are results for the nonspin-polarized case. We find that the effect of spin polarization in the case of LDA is very small while for GGA it significantly decreases the value of α . At room temperature, the lattice parameter for NSP Ni is only $\sim 0.3\%$ smaller than for the SP case, for both LDA and GGA. Such a comparison is not possible for Fe since calculating the thermal expansion for NSP bcc Fe would be meaningless, given the presence of unstable phonon modes.

The temperature range at which the calculated and experimental values of $\alpha(T)$ start to diverge corresponds to the range of temperatures at which the magnetic moments begin to disorder, prior to the transition from ferromagnetic to paramagnetic behavior. This effect is difficult to incorporate in calculations. The free energy would need to include the entropy terms due to disordered spins, as well as the effect of disordered spins on the lattice constant. We note that the effect of reducing magnetization due to disordered spins is quite different from that due to ordered spins whose individual moment decreases. In the latter case, the lattice constant should decrease, whereas the former leads to an increase. Thus, the constrained magnetization approach of Sec. III B cannot illuminate the question of α 's dependence on magnetization.

Figures 9 and 10 show how B_0 and B'_0 vary with temperature. The experimental data are only available for room temperature, as shown in Table I. We can however compare the LDA and GGA values as a function of temperature; we find that ΔB_0 is $\sim 40\%$ for Fe at all temperatures, and for Ni ranges from 25% to 27% in the temperature range shown.

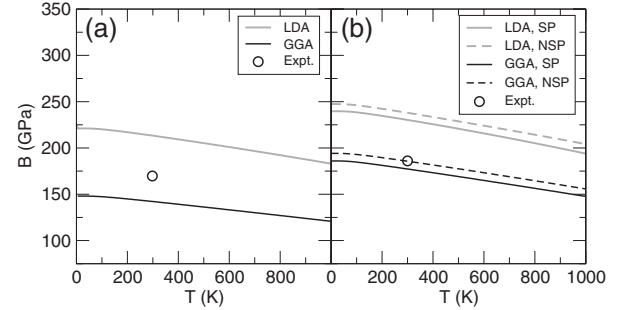


FIG. 9. Calculated values for the temperature dependence of the bulk modulus for (a) Fe and (b) Ni. For Ni, results from both SP and NSP calculations are presented. The experimental values are from Ref. 17.

The agreement between LDA and GGA is better for B' but is more strongly temperature dependent: $\Delta B'_0$ ranges from 15% to 22% for Fe and 1.3% to 11% for Ni.

IV. CONCLUSIONS AND SUMMARY

The main message of this paper is that the presence of magnetism considerably complicates any consideration of exchange-correlation errors at harmonic and anharmonic orders. To summarize, for the nonmagnetic metals the lessons learned from previous calculations are that (i) harmonic and thermal properties are most accurately predicted by an XC functional that gets $a_0(0)$ closest to experiment and (ii) errors in anharmonic quantities are negligible. In the present work we find that while conclusion (i) still holds for magnetic metals, conclusion (ii) fails. This is because, in the case of magnetic metals, the relevant phase space for determination of thermal properties is a function of not one parameter, (a_0), but two (a_0, m_0). Therefore, derivatives may be evaluated not just at an a_0 that is incorrect, due to XC errors, but also at an incorrect magnetization. The high-temperature properties of magnetic metals are thus difficult to compute accurately due to both the disordering of magnetic moments and also the increasing importance of anharmonic quantities.

For static properties, such as the bulk modulus and its pressure derivative, the error at anharmonic order is less than

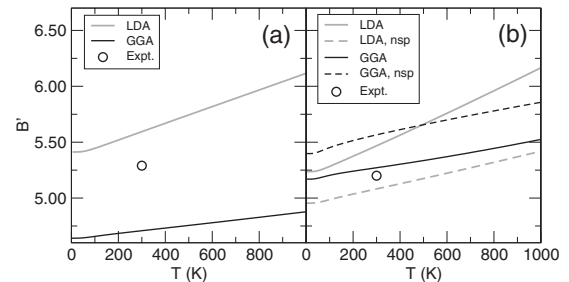


FIG. 10. Calculated values for the temperature dependence of the pressure derivative of the bulk modulus for (a) Fe and (b) Ni. For Ni, results from both SP and NSP calculations are presented. The experimental values are from Refs. 17 and 18, respectively.

at harmonic order, but only by a factor of ~ 2 , rather than the factor of ~ 10 typical of the nonmagnetic metals. Interestingly, the presence of magnetism appears to have much greater effect on B_0 than on B'_0 . In contrast to the nonmagnetic metals, the GGA performs considerably better than the LDA, leading to more accurate lattice constants. As predicted by the trends seen in nonmagnetic metals, the GGA also gives a better description of thermal properties than the LDA. However, at temperatures where the disordering of magnetic moments becomes evident, the simple spin-polarized quasiharmonic treatment of thermal expansion

does not suffice, and the coefficient of thermal expansion is underestimated.

ACKNOWLEDGMENTS

This work was partially supported by the IMI Program of the National Science Foundation under Award No. DMR04-09848. Helpful discussions with Nicola Spaldin, Stefano de Gironcoli, and Madhura Marathe are gratefully acknowledged.

-
- ¹S. Narasimhan and S. de Gironcoli, *Phys. Rev. B* **65**, 064302 (2002).
- ²A. A. Quong and A. Y. Liu, *Phys. Rev. B* **56**, 7767 (1997).
- ³J. Xie, S. de Gironcoli, S. Baroni, and M. Scheffler, *Phys. Rev. B* **59**, 965 (1999).
- ⁴B. Grabowski, T. Hickel, and J. Neugebauer, *Phys. Rev. B* **76**, 024309 (2007).
- ⁵D. J. Kim, *New Perspectives in Magnetism of Metals* (Springer, New York, 1999).
- ⁶J.-H. Lee, Y.-C. Hsue, and A. J. Freeman, *Phys. Rev. B* **73**, 172405 (2006).
- ⁷F. Körmann, A. Dick, B. Grabowski, B. Hallstedt, T. Hickel, and J. Neugebauer, *Phys. Rev. B* **78**, 033102 (2008).
- ⁸Y. Nakamura, *IEEE Trans. Magn.* **12**, 278 (1976).
- ⁹D. Alfè, G. Kresse, and M. J. Gillan, *Phys. Rev. B* **61**, 132 (2000).
- ¹⁰S. Baroni *et al.*, <http://www.pwscf.org/>
- ¹¹J. P. Perdew and A. Zunger, *Phys. Rev. B* **23**, 5048 (1981).
- ¹²J. P. Perdew, K. Burke, and M. Ernzerhof, *Phys. Rev. Lett.* **77**, 3865 (1996).
- ¹³Specific pseudopotentials used are Fe.pbe-nd-rrkjus.UPF and Ni.pz-nd-rrkjus.UPF, both available on the QUANTUM ESPRESSO website.
- ¹⁴F. Birch, *Phys. Rev.* **71**, 809 (1947).
- ¹⁵F. C. Nix and D. MacNair, *Phys. Rev.* **60**, 597 (1941).
- ¹⁶Z. S. Basinski, W. Hume-Rothery, and A. L. Sutton, *Proc. R. Soc. London, Ser. A* **229**, 459 (1955).
- ¹⁷C. Kittel, *Introduction to Solid State Physics*, 8th ed. (Wiley, New York, 2005).
- ¹⁸P. Lazor, Ph.D. thesis, Uppsala University, 1993.
- ¹⁹The $6 \times 6 \times 6$ k -point grid used here has been verified to give sufficiently converged results for total energies, lattice parameters, and phonon frequencies, and thus also for thermal expansion. However, the magnetic moment for Ni does change upon using a denser k -point mesh, and for a $10 \times 10 \times 10$ k -point grid the values obtained are $0.61 \mu_B$ and $0.63 \mu_B$ for LDA and GGA, respectively.
- ²⁰J. Paul and S. Narasimhan, *Bull. Mater. Sci.* **31**, 569 (2008).
- ²¹R. Pushpa, U. Waghmare, and S. Narasimhan, *Phys. Rev. B* **77**, 045427 (2008).
- ²²B. N. Brockhouse, H. E. Abou-Helal, and E. D. Hallman, *Solid State Commun.* **5**, 211 (1967).
- ²³A. Dal Corso and S. de Gironcoli, *Phys. Rev. B* **62**, 273 (2000).
- ²⁴R. J. Birgeneau, J. Cordes, G. Dolling, and A. D. B. Woods, *Phys. Rev.* **136**, A1359 (1964).
- ²⁵E. C. Stoner, *Proc. R. Soc. London, Ser. A* **165**, 372 (1938).
- ²⁶H. C. Herper, E. Hoffmann, and P. Entel, *Phys. Rev. B* **60**, 3839 (1999).
- ²⁷X. Sha and R. E. Cohen, *Phys. Rev. B* **73**, 104303 (2006).